

## Electronic Supplementary Information

### Studies on PVDF/Ferrite composite films on flexible substrate for pyroelectric energy conversion

Achal Bhiogade<sup>1,2</sup>, Katragadda Nagamalleswari<sup>3</sup>, Pranab Mandal<sup>3‡</sup> and Vengadesh Kumara Mangalam Ramakrishnan<sup>1\*</sup>

<sup>1</sup>Functional Materials Laboratory, Department of Chemistry, Faculty of Engineering and Technology, SRM Institute of Science and Technology, Kattankulathur-603203, Tamil Nadu, India

<sup>2</sup>Department of Physics and Nanotechnology, Faculty of Engineering and Technology, SRM Institute of Science and Technology, Kattankulathur-603203, Tamil Nadu, India

<sup>3</sup>Department of Physics, SRM University – AP, Amaravati, 522 240, Andhra Pradesh, India.

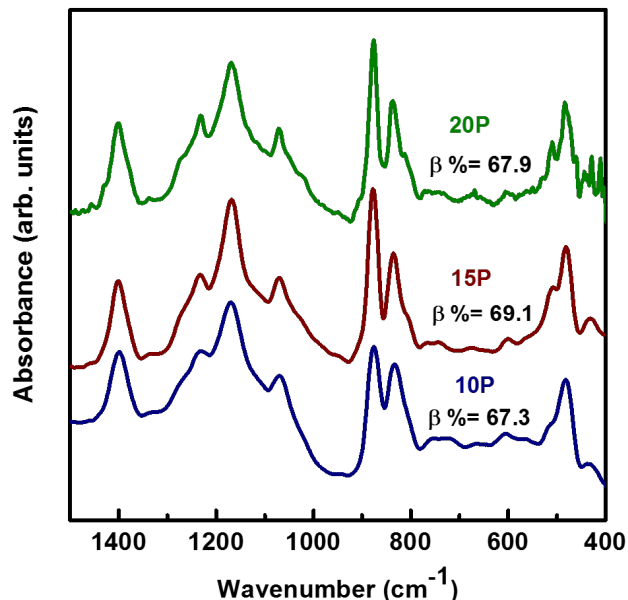
‡ Email: pranab.m@srmmap.edu.in

\*Email: vengader@srmist.edu.in

#### Table of Contents

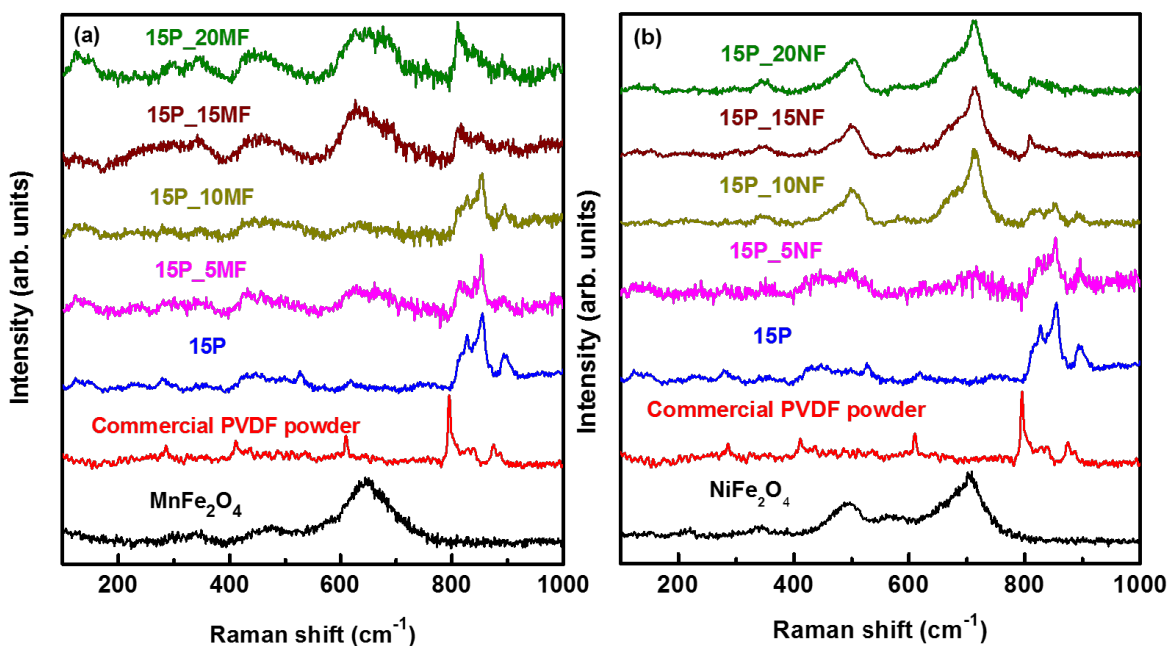
1. Phase analysis .....	2
2. Morphology studies .....	4
3. Magnetic studies .....	4
4. Ferroelectric measurement .....	5

## 1. Phase analysis



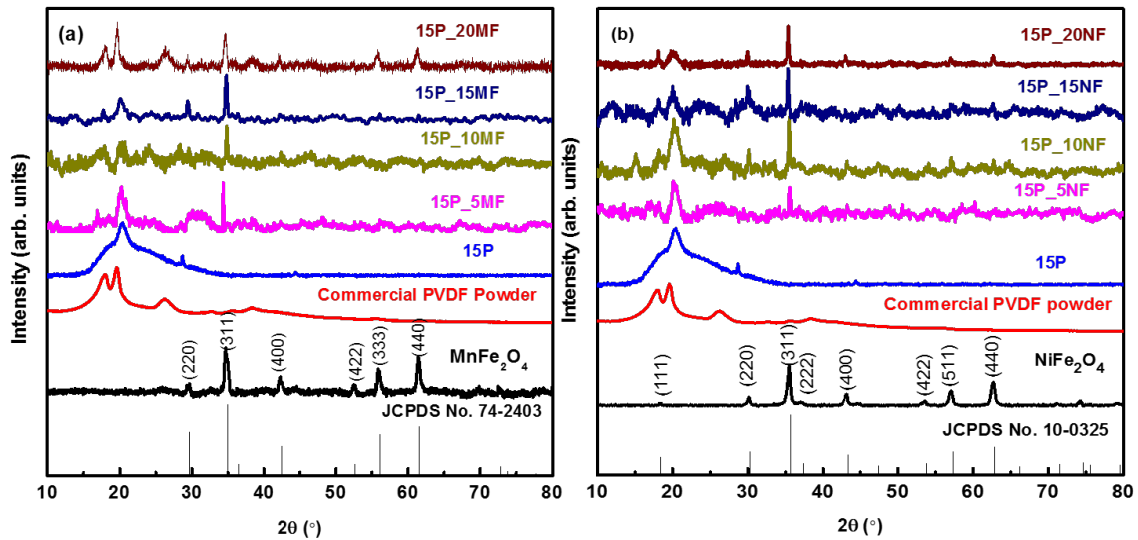
**Figure S1.** FTIR spectra of 10, 15, 20 % concentration of PVDF films

FTIR spectra (Figure S1) reveal three different concentrations of PVDF (10, 15, 20 w/v %). Figure S1 FTIR spectra show that the 15% concentration of PVDF film has a higher  $\beta$ -phase than the 10 and 20 % concentration of PVDF films.<sup>1</sup>



**Figure S2.** Raman spectra of (a) MnFe<sub>2</sub>O<sub>4</sub> and PVDF/MnFe<sub>2</sub>O<sub>4</sub> (b) NiFe<sub>2</sub>O<sub>4</sub> and PVDF/NiFe<sub>2</sub>O<sub>4</sub> composite films

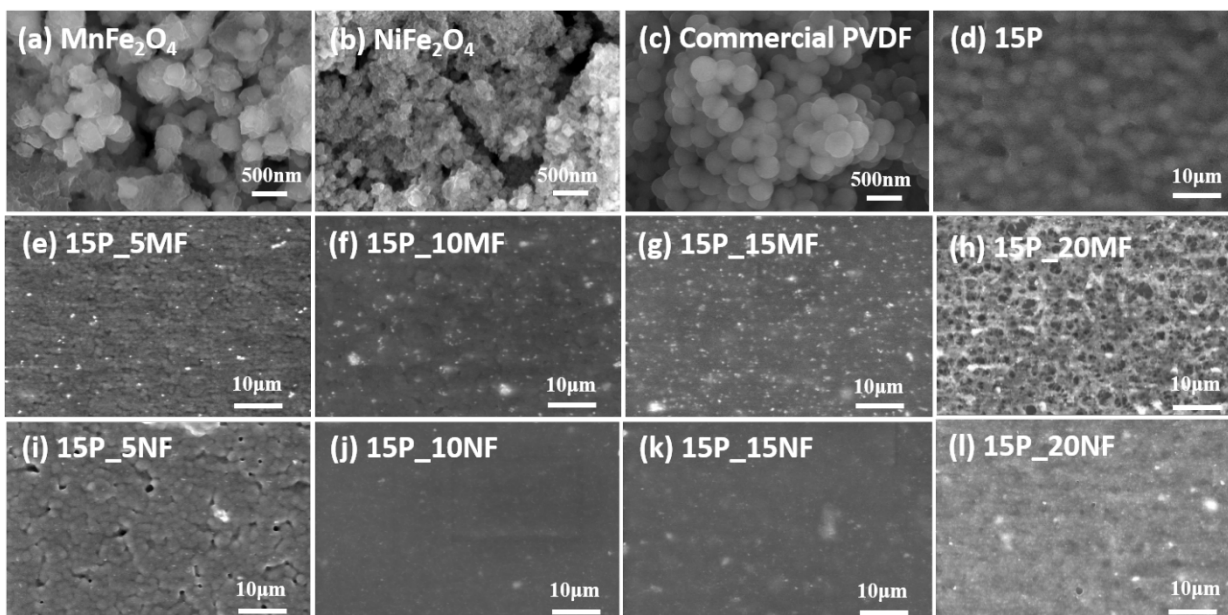
Raman spectra for synthesized  $\text{MnFe}_2\text{O}_4$ ,  $\text{NiFe}_2\text{O}_4$ , commercial PVDF powder, PVDF film and PVDF composite films were recorded by using the Micro Raman spectrometer Horiba, LABRAM HR Evolution at room temperature (Figure S2). The Raman band at 473 and 647  $\text{cm}^{-1}$  indicates the tetrahedral and octahedral sites of  $\text{MnFe}_2\text{O}_4$ . The Raman band appeared at 490 and 700  $\text{cm}^{-1}$ , indicating the tetrahedral and octahedral sites of  $\text{NiFe}_2\text{O}_4$ .<sup>2</sup> Raman spectrum of commercial PVDF powder shows the presence of the  $\alpha$ -phase, which has peaks at 283, 410, 535, 610, and 795  $\text{cm}^{-1}$ . PVDF/ $\text{MnFe}_2\text{O}_4$  and PVDF/ $\text{NiFe}_2\text{O}_4$  composite films indicate that the Raman bands at 263, 510, and 839  $\text{cm}^{-1}$  lead to the formation of the  $\beta$ -phase.<sup>1,3</sup> As shown in Figure S2, the intense peak of PVDF powder at 795  $\text{cm}^{-1}$  indicates the presence of  $\alpha$ -phases, but  $\alpha$ -phase is reduced in PVDF film and PVDF composite films by increasing the intensity of  $\beta$ -phase peak at 839  $\text{cm}^{-1}$ . As the concentration of fillers increases, the intensity of the  $\beta$ -phase peak decreases, and strong ferrite bands appear in the composite films (Figure S2(a, b)). These results supported FTIR spectra; as the concentration of fillers increases above a certain level, the  $\beta$ -phase is reduced, which may cause due to agglomeration of particles in the composite films.



**Figure S3.** X-ray diffraction pattern of a) PVDF/ $\text{MnFe}_2\text{O}_4$  b) PVDF/ $\text{NiFe}_2\text{O}_4$  composite films

Figure S3 reveals the X-ray diffraction pattern of PVDF/ $\text{MnFe}_2\text{O}_4$ , PVDF/ $\text{NiFe}_2\text{O}_4$  composite films along with PVDF film, commercial PVDF powder,  $\text{MnFe}_2\text{O}_4$  and  $\text{NiFe}_2\text{O}_4$  powder.

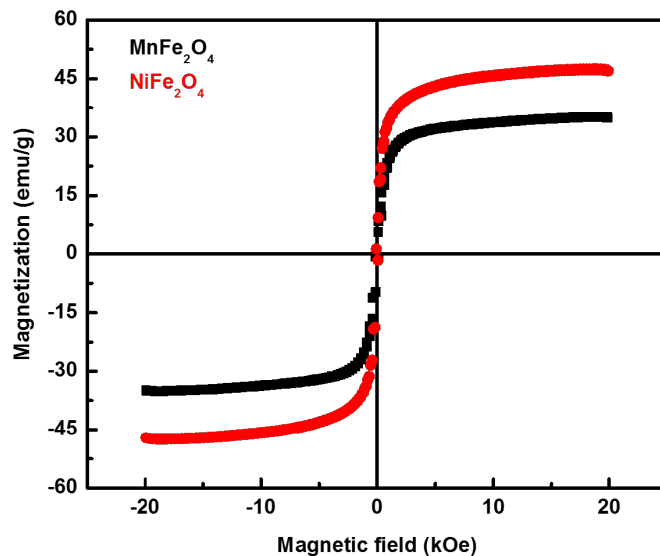
## 2. Morphology studies



**Figure S4.** Scanning electron micrograph of (a)  $\text{MnFe}_2\text{O}_4$  (b)  $\text{NiFe}_2\text{O}_4$  (c) commercial PVDF powder (d) 15P (e) 15P\_5MF (f) 15P\_10MF (g) 15P\_15MF (h) 15P\_20MF (i) 15P\_5NF (j) 15P\_10NF (k) 15P\_15NF (l) 15P\_20NF

Figure S4 reveals the scanning electron micrographs obtained for PVDF/ $\text{MnFe}_2\text{O}_4$ , PVDF/ $\text{NiFe}_2\text{O}_4$  composite films along with PVDF film, commercial PVDF powder,  $\text{MnFe}_2\text{O}_4$  and  $\text{NiFe}_2\text{O}_4$  powder.

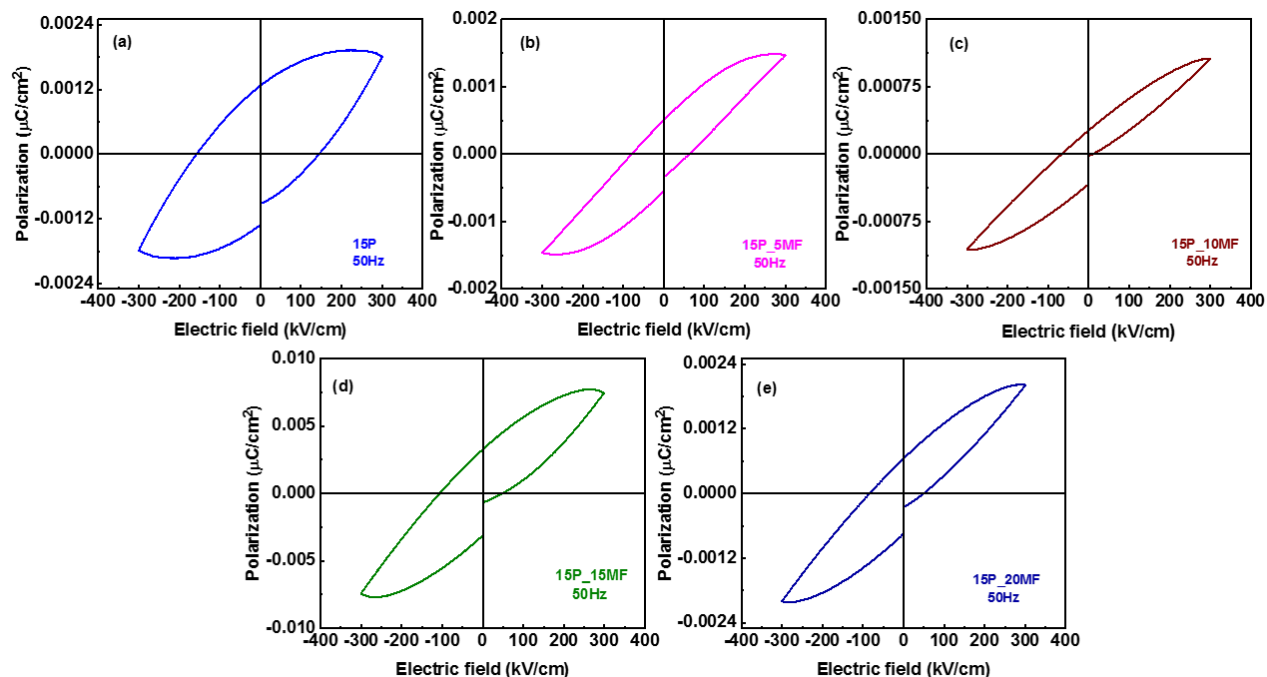
## 3. Magnetic studies



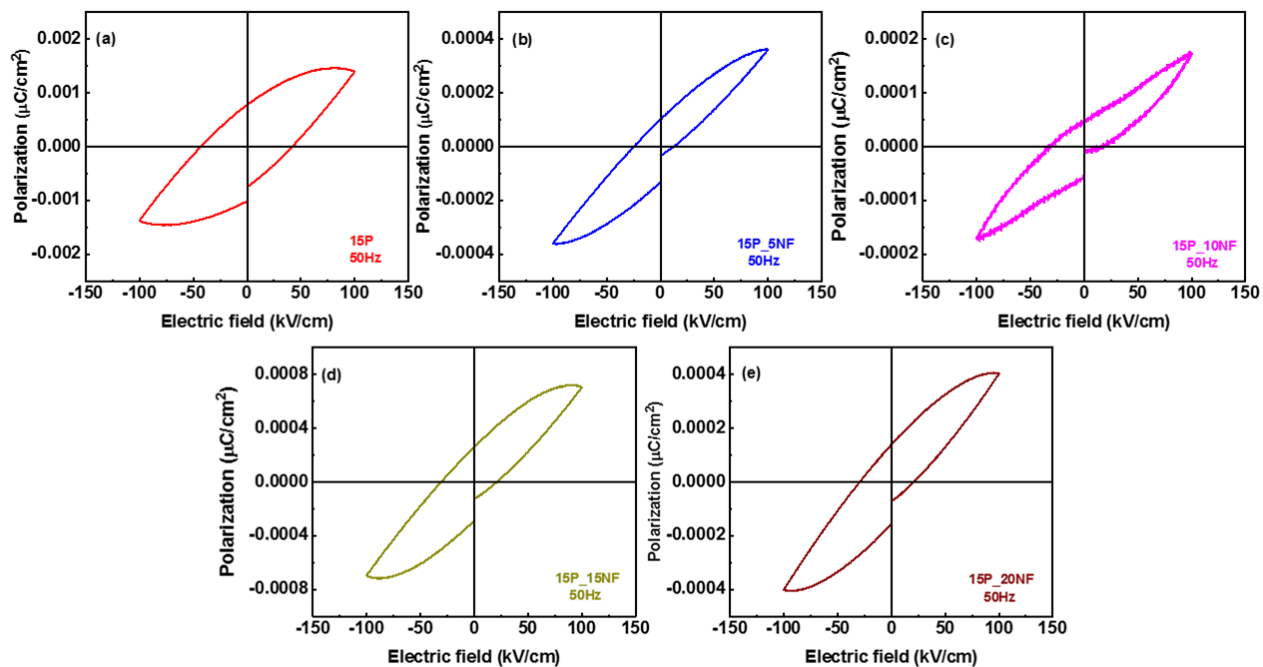
**Figure S5.** Magnetic hysteresis loop of synthesized  $\text{MnFe}_2\text{O}_4$  and  $\text{NiFe}_2\text{O}_4$  powder.

Figure S5 reveals the room temperature magnetic hysteresis loop obtained for synthesized  $\text{MnFe}_2\text{O}_4$  and  $\text{NiFe}_2\text{O}_4$  powder.

#### 4. Ferroelectric measurement



**Figure S6.** Ferroelectric hysteresis loop of (a) PVDF film (b-e) PVDF/ $\text{MnFe}_2\text{O}_4$  composite films



**Figure S7.** Ferroelectric hysteresis loop of (a) PVDF film (b-e) PVDF/ $\text{NiFe}_2\text{O}_4$  composite films

The ferroelectric hysteresis loop of PVDF film, PVDF/MnFe<sub>2</sub>O<sub>4</sub>, and PVDF/NiFe<sub>2</sub>O<sub>4</sub> composite films are shown in Figures S6 and S7.

## References

1. A. Bhiogade, K. Nagamalleswari, P. Mandal and R. V. K. Mangalam, *J. Polym. Res.*, 2023, **30**, 288.
2. R. B. Kamble, V. Varade, K. Ramesh and V. Prasad, *AIP Adv.*, 2015, **5**.
3. C. Constantino, A. Job, R. Simoes, J. Giacometti, V. Zucolotto, O. Oliveira Jr, G. Gozzi and D. Chinaglia, *Appl. spectrosc.*, 2005, **59**, 275-279.